ISBN: 978-3-95450-234-9 ISSN: 2673-5504 doi:10.18429/JACoW-SRF2023-WEPWB049

MULTIPACTING IN C75 CAVITIES*

G. Ciovati†, P. Dhakal, R. Rimmer, H. Wang, S. Wang, Jefferson Lab, Newport News, VA, USA

Abstract

Cavities for the C75 CEBAF cryomodule refurbishment program are currently being built, processed, tested and installed in the CEBAF accelerator at Jefferson Lab. They consist of 5-cell, 1497 MHz cavities with waveguide-type power coupler and for higher-order modes. Most of the cavities' RF tests in a vertical cryostat at 2.07 K were limited by strong multipacting at accelerating gradients in the range 18 – 23 MV/m. A softer multipacting barrier was sometimes encountered at 13 – 15 MV/m. An unusual feature of the multipacting was that the barrier often shifted to a lower gradient ~ 17 MV/m, after multiple quenches at ~ 20 MV/m. This phenomenon was reproduced in a single-cell cavity of the same shape. The cavity was tested after different amounts of mechanical tuning and different amounts of residual magnetic field, with no significant impact to the multipacting behavior. This contribution summarizes the experimental results from cavity RF tests, some of which were complemented by additional diagnostic instrumentation, such as oscillating superleak transducers, flux-gate magnetometers and temperature sensors. Results from 2D and 3D simulations are also presented, indicating favorable conditions for multipacting at the equator in the range 20 – 29 MV/m.

INTRODUCTION

One of the current cryomodule refurbishment programs at Jefferson Lab aims at replacing the lowest performing original cavities, installed in the CEBAF accelerator in the 1990s, with cells of a different shape with a target operational accelerating gradient, E_{acc} of 19.1 MV/m, with a quality factor $Q_0 \geq 8 \times 10^9$ at 2.07 K [1]. The 5-cell cavities are being fabricated by Research Instruments (RI), GmbH, Germany and 36 cavities have been fabricated since 2019. Eight 5-cell cavities are installed in each refurbished cryomodule which has a target energy gain of 75 MeV, hence the name "C75" to the cryomodule type. Two such cryomodules, C75-01 and -02, have been operating in CEBAF since June 2021 and the results are presented in Ref. [2].

The cell shape is the same as the one designed for a high-current free-electron laser [3, 4]. 2D multipacting (MP) simulations indicated that any MP barrier should occur at E_{acc}-values well above 20 MV/m [5]. Several single- and 5-cell prototype cavities were fabricated and tested as part of that project. No significant issues with MP was found, although two of the three 5-cell cavities were limited to E_{acc} ~20 MV/m [6–8].

The cavities' surface treatments are all done at Jefferson Lab and two options were pursued: the first option consisted of bulk removal (100 µm) by electropolishing (EP) followed by annealing at 800 °C for 3 h, followed by a final 30 µm EP. The second option consisted of 60 µm removal by centrifugal barrel polishing (CBP) and 40 µm EP for bulk removal, 800 °C for 3 h, followed by a final 30 µm EP.

The equator weld-prep for cells used for C75-01 cavities (with serial numbers 5C75-RI-001 to -008) was only 5.2 mm wide and resulted in sharp grain boundary steps intercepting the equatorial weld, which was a cause of concern for possible premature quenching due to local field enhancement. To eliminate such concern, the width of a cell's equator weld-prep was increased to 1.3 cm for all the remaining cavities.

The cryogenic RF tests of the cavities in a vertical dewar at Jefferson Lab showed that MP was the dominant limitation to the performance of the C75 cavities [9]. An unusual feature of the MP was that, after multiple MP-induced quenches, the barrier sometimes shifted to a lower gradient ~ 17 MV/m, and could not be rf processed quickly. The phenomenon could be reproduced by thermally cycling the cavity to ~ 20 K. It should be noted that two C75 cavities made of standard, high-purity, fine-grain Nb were also built by RI for Nb_3Sn coating studies and one achieved 23 MV/m while the other reached 28 MV/m [10].

Besides differences in the equator weld-prep geometries and surface preparation, we investigated the impact of changes in the cavity shape by mechanical tuning of a single-cell cavity. The following Sections described some of the experimental results and multipacting simulations.

EXPERIMENTAL RESULTS

Five-Cell Cavities

The results from the initial cryogenic RF test of cavity 5C75-RI-013 shown in Fig. 1 have been observed in many C75-type cavities: the cavity reached ~ 20.5 MV/m, then after several multipacting-induced breakdown events, the cavity broke-down at ~ 17 MV/m, with no improvement after ~ 30 min RF processing. The same behavior is reproduced after thermally cycling the cavity to ~ 20 K. Oscillating superleak transducers (OSTs) were mounted on the test stand to aid locating the breakdown location, which was found to be in the middle cell, ~ 5 cm away from the equator weld, for the barrier at ~ 17 MV/m. The cavity was processed by CBP.

The cavity was baked, while on the test stand, at 120 °C for 48 h and re-tested. The breakdown was now stable at ~ 20.5 MV/m and the location was at the equator of the middle cell. The test stand was equipped with a needle-valve and a high-purity He gas bottle and He processing for attempted to overcome the MP barrier. The maximum gradient increased by ~ 1.5 MV/m following He processing for ~ 1.5 h, as shown in Fig. 1. No radiation due to field-emitted electrons was detected on top of the test stand during any of the tests shown in Fig. 1

* This work was supported by Jefferson Science Associates, LLC under U.S. DOE Contract No. DE-AC05-06OR23177.
† gciovati@jlab.org

ISBN: 978-3-95450-234-9 ISSN: 2673-5504 doi:10.18429/JACoW-SRF2023-WEPWB049

The MP location at ~ 17 MV/m being in the middle cell at ~ 5 cm away from the equator weld was confirmed for two other cavities for which the test stand was instrumented with OSTs.

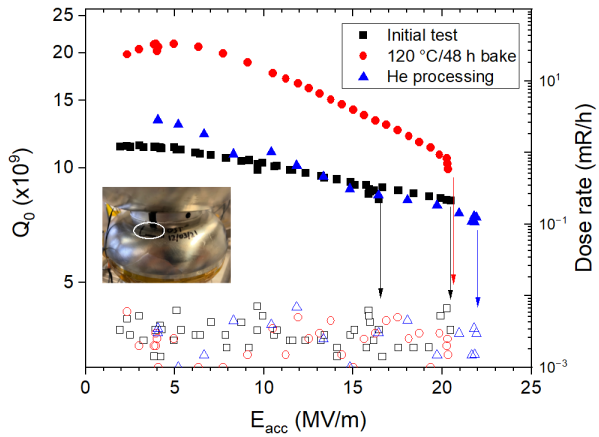

Figure 1: $Q_0(E_{acc})$ measured at 2.07 K for cavity 5C75-RI-013 during the initial RF test, after low-temperature baking and after He processing. The arrows represent the breakdown field for each test. The inset shows a picture of the MP location at ~ 17 MV/m found during the initial test, circled in white.

Figure 2 shows the $Q_0(E_{acc})$-curves measured at 2.07 K for cavities 5C75-RI-031 and 5C75-RI-032, assembled as a "cavity-pair". The data show a behavior similar to that found during the initial test of cavity 5C75-RI-013: the breakdown field in both cavities is reduced to 15 – 17 MV/m after a few breakdown events at ~ 19 MV/m. The same behavior was reproduced after thermally cycling the cavity pair to ~ 20 K. Both cavities were processed by bulk EP.

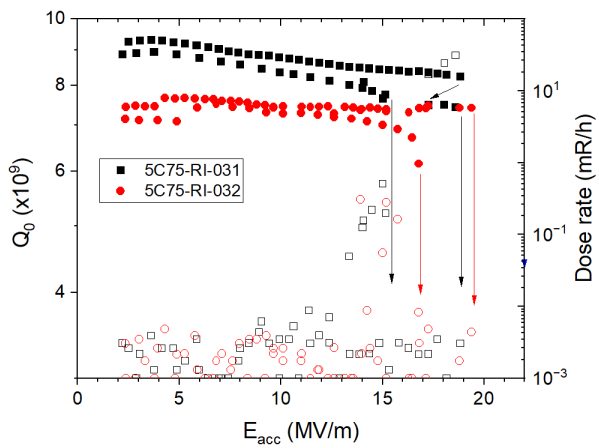

Figure 2: $Q_0(E_{acc})$ measured at 2.07 K for cavities 5C75-RI-031 and -032 in a "cavity-pair" configuration. The arrows represent the breakdown field for each cavity, reducing from ~ 19 MV/m to ~ 16 MV/m.

Of all the cavity-pair tested so far, 3 out of 8 cavities for both cryomodules C75-01 and C75-02 and 2 out of 2 cavities for C75-04 showed the unusual MP behavior discussed above. In order to avoid the possibility of MP-induced breakdown below the target E_{acc}, after MP at higher gradient, a administrative limit of 21 MV/m was set for cavities tested both in the vertical cryostat and inside cryomodules. No significant difference in the cavities performance has emerged thus far regarding the bulk removal method or the equator weld-prep geometry. So far, 6 out of 11 cavities processed by EP only have reached the administrative limit and 7 out of 11 of 11 cavities processed by CBP and EP have reached the administrative limit.

Cavity-pairs are cooled-down to 2.07 K under static vacuum conditions, whereas a cavity is actively pumped on a test-stand for single-cavity tests. Figure 3 shows an example of the partial pressure of the residual gases in the cavity-pair test stand after assembly and evacuation of different cavity pairs. The performance of pairs RI031-RI032 (shown in Fig. 2) and RI022-RI025 were clearly limited by multipacting, whereas that of RI019-RI020 and RI011-RI018 reached 21 MV/m. In general, a peak at atomic mass unit of 64, associated with sulfur dioxide [11], was present for all cavities, in the range 2.3×10^{-10} Pa to 1.7×10^{-8} Pa. This peak is associated with residual sulfur from the EP process. However, no strong correlation between the partial pressure of SO_2 and the occurrence of MP has emerged thus far.

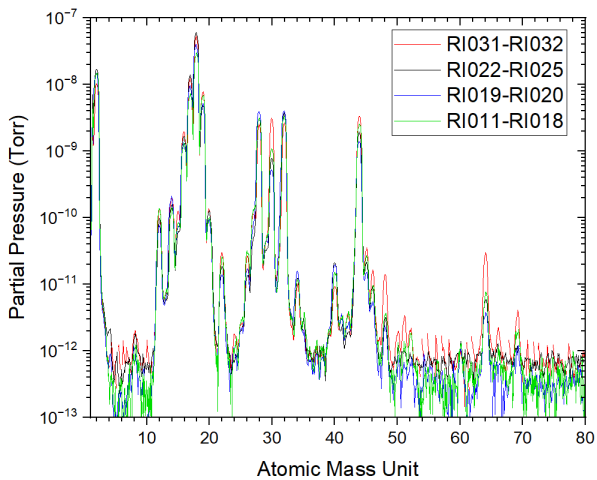

Figure 3: Spectra of the residual gases measured for several C75 cavity-pairs.

Single-Cell Cavity

The single-cell cavity C75-SC3 with the same cell shape as that of the inner cell of the 5-cell cavity was built at Jefferson Lab from medium-grain Nb with *RRR* ~ 100. The sequence of surface processing and cryogenic RF tests at 2 K are listed in Table 1 and the $Q_0(E_{acc})$-curves for tests 1-4 can be found in Ref. [12]. The cavity achieved a maximum accelerating gradient, E_{max}, of 34.3 MV/m in test No. 2. All the tests were limited by MP-induced quenches and the MP barrier dropped to a lower gradient after quenching, with no field emission. Single-axis cryogenic flux-magnetometers (FGMs) and temperature sensors were attached to the cavity

ISBN: 978-3-95450-234-9 ISSN: 2673-5504 doi:10.18429/JACoW-SRF2023-WEPWB049

for all tests. OSTs were attached to the test-stand for tests No. 4 and 6, locating the MP location to be at the equator of the cavity.

The cavity was kept under static vacuum conditions for tests No. 4-7 and mechanical tuning, in both tension and compression, was done to alter the cavity shape and evaluate the effect on the MP barrier. The frequency shift measured at 295 K after each tuning session is listed in Table 1. A 3D laser scanner was used to measure the shape of the outer surface of the cavity. Figure 4 shows a color map of the deviation between the cavity outer surface measured after the last tuning listed in Table 1 and the nominal outer surface. The nominally flat walls acquired an angle of ~ 20 °C and the cell length was stretched by ~ 11 mm.

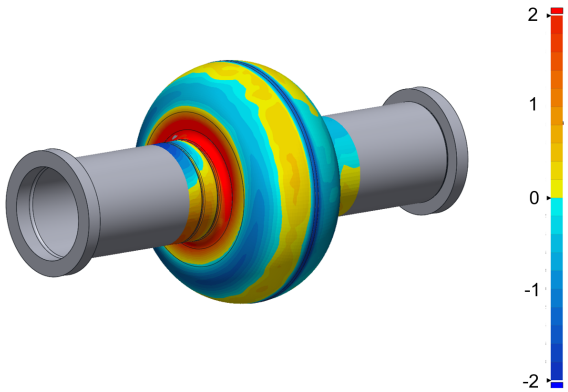

Figure 4: 3D comparison between the outer surface measured after stretching C75-SC3, resulting in a frequency shift of ~ 23 MHz, and the nominal outer surface. The values in the color bar are in mm.

Figure 5 shows the $Q_0(E_{acc})$ measured during test 5, showing a degradation of Q_0 after the first and subsequent MP-induced quenches. This degradation correlates with jumps in magnetic flux detected by a FGM near the quench location. Higher temperature was also measured by one sensor near the MP/quench location, identified to be ~ 1 cm off the equator. The ambient magnetic field was increased from ~ 1 mG to ~ 30 mG while the cavity was MP, but it had no effect on the MP barrier. Similar behavior was observed during tests No. 6 and 7. The $Q_0(E_{acc})$ measured during test 7 is also shown in Fig. 5 and the local temperature and magnetic field near the MP/quench location are shown in Fig. 6, clearly showing the trapping of magnetic flux in the cavity wall, resulting in the reduced Q_0. FGMs 1 and 3 are aligned along the cavity axis, whereas FGM2 is tangential to the equator circumference. As part of test No. 7, the cavity was warmed-up above 9.2 K and slow-cooled in a residual magnetic field of 20 mG. The cavity was able to reach 23 MV/m during the initial power rise but after the first few MP-induced quenches, the cavity was limited to 18.8 MV/m.

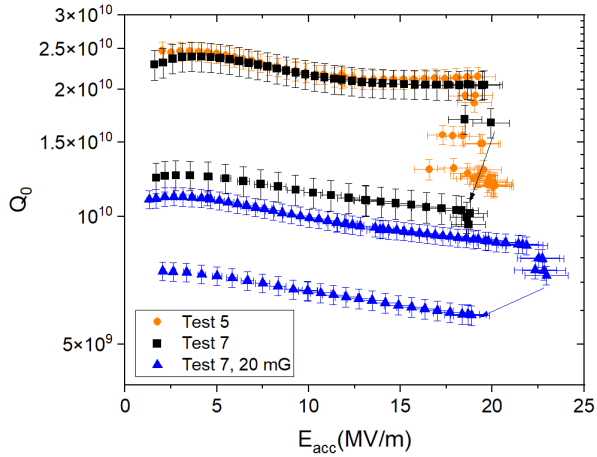

Figure 5: $Q_0(E_{acc})$ measured at 2 K for single-cell cavity C75-SC3 during tests 5 and 7.

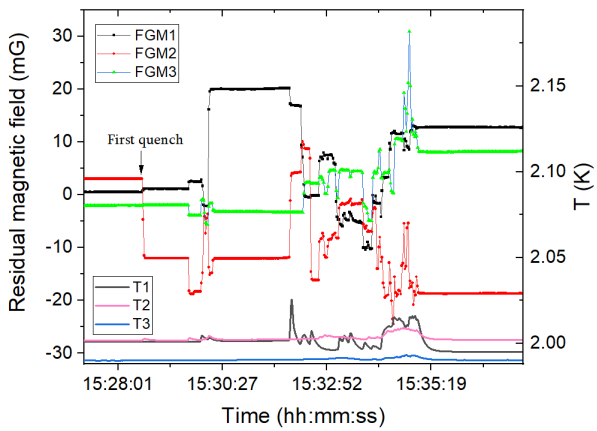

Figure 6: Local temperature and magnetic field measured near the MP-induced quench location measured for single-cell cavity C75-SC3 at 2 K during test 7, after cool-down in ~ 1 mG residual magnetic field.

MULTIPACTING SIMULATIONS

2D MP simulations were repeated using FishPact [13] for center-cell and end-cell geometries with Dirichlet boundary conditions at the irises, with and without different equator weld-preps used for cavity fabrication. The calculations were made assuming an initial energy of both the primary and secondary electron of 2 eV and the electron trajectory was tracked up to 20 impacts to the surface. The code assumes that the emission angle of the secondary electron is normal to the surface. The results showed that there are many emission sites, distributed over the entire profile, and many phases of the RF field resulting in 2-point resonant trajectories at the equator.

Figure 7 shows the average final electron energy as a function of the accelerating gradient. Considering the low-energy threshold for the secondary emission yield (SEY) > 1 to be ~25 eV for unbaked Nb [14], the results in Fig. 7 could be interpreted as a low probability for any strong MP in C75 cavities below ~25 MV/m.

ISBN: 978-3-95450-234-9 ISSN: 2673-5504 doi:10.18429/JACoW-SRF2023-WEPWB049

Table 1: Summary of RF Test Results Following Different Surface Treatment and Tuning Applied to the C75 Single-cell Cavity C75-SC3

Test No.	E_{max} (MV/m)	Treatment	Comment
1	29.5	120 µm EP, 650 °C/10 h, 25 µm EP	E_{max} dropped to 26.5 MV/m after quench. No Q_0-degradation after quench.
2	34.3	120 °C/48 h	E_{max} dropped to 28 MV/m after quench. No Q_0-degradation after quench.
3	31.9	60 µm CBP, 30 µm EP, 800 °C/3 h, 25 µm EP	E_{max} dropped to 26.8 MV/m after quench. Q_0 degraded after quench.
4	21.5	1000 °C/3 h	E_{max} dropped to 17.7 MV/m after quench. Q_0 degraded after quench.
5	19.3	-300 kHz mechanical tuning	E_{max} dropped to 16.8 MV/m after quench, processed up to 20.4 MV/m with lower Q_0.
6	19.8	-1.284 MHz mechanical tuning	E_{max} dropped to 15.7 MV/m after quench, processed up to 23.5 MV/m with lower Q_0, dropped back to 20 MV/m after quenching.
7	20.0	+22.887 MHz mechanical tuning	E_{max} dropped to 18.7 MV/m after quench with lower Q_0.
8	30.3	25 µm EP	E_{max} dropped to 26.3 MV/m after quench. No Q_0-degradation after quench.

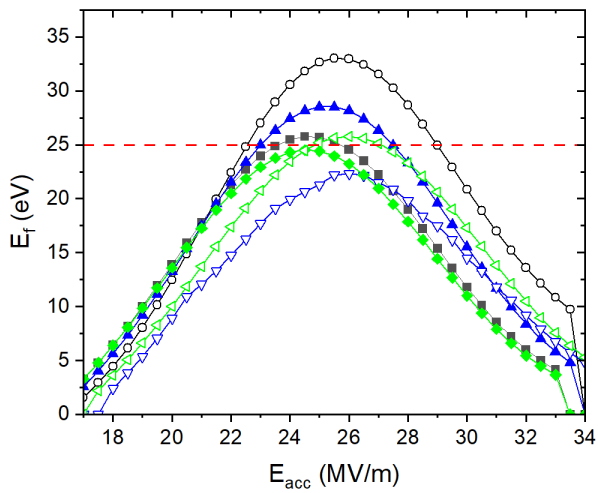

Figure 7: Average final impact energy of electrons making 20 impacts to the surface as a function of E_{acc} calculated with FishPact for the nominal cell shape, with no weld-prep (black symbols), with the weld-prep for cavities used in cryomodule C75-01 (blue symbols) and with the weld-prep for cavities used for C75-02 and beyond. Solid symbols are for the center-cell shape, empty symbols are for the end-cell shape. The dashed line represents the threshold for SEY > 1 for unbaked Nb.

3D MP simulations were carried out using ACE3P [15] on both a full-scale model of the 5-cell cavity and on a single-cell cavity with beam tubes. The cell geometry was created from the 2D profile of a half-cell measured with a coordinate measuring machine at RI. The measured half-cell was welded into a dumb-bell with stiffening rings and prior to machining of the equator weld-prep. The deviation from the nominal profile was less than 200 µm. The nominal geometry of the weld-prep used for C75-02 cavities was included in the 3D geometry of the cavity used for the simulation.

Figure 8 shows the geometry of the 5-cell cavity used for the simulation and details of the equator weld-preps for the inner cells and end-cells. In order to capture the possible effects from the small geometrical features of the weld-prep on resonant trajectories near the surface, a finer meshed strip is defined along the cell profile. The primary electrons are emitted normal to the surface from a region inside and near this strip. The finer mesh also allows for a more dense distribution of emitting sites, since ACE3P will launch initial electrons from each mesh element when computing with ElectronicSurface type.

Figure 9 shows an example of a few electron trajectories ending in a resonant 2-point MP loop at the equator. About six thousands trajectories have been produced and resonances only happens at the equator. For the 5-cell cavity model, more than 11,000 trajectories are produced for each of the end cells. Electrons could travel to other cells, potentially triggering MP there.

The existence of resonant trajectories was confirmed by tracking electrons for many RF periods. In our simulation, we tracked 100 RF cycles, and clearly found resonances with stable impact energies and resonance loop. Figure 10 shows the final impact energy as a function of E_{acc} for electrons tracked for up to 9 RF periods, making at least 20 impacts and for initial energies of the secondary electron of 2 eV and 4 eV. The plot shows that if the initial energy were to be 4 eV, favorable conditions for MP could occur between ~19 MV/m and ~22 MV/m, depending on the cell.

ISBN: 978-3-95450-234-9 ISSN: 2673-5504 doi:10.18429/JACoW-SRF2023-WEPWB049

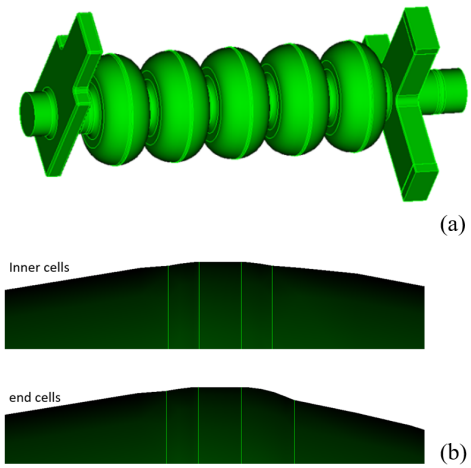

Figure 8: 3D geometry of the 5-cell cavity used for MP simulations with ACE3P (a) and details of the equator weld-prep geometry (b).

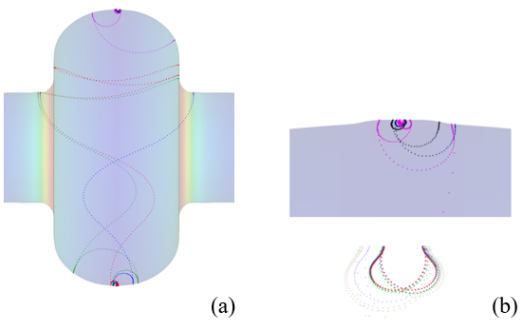

Figure 9: Example of resonant trajectories found in the single-cell model with the C75 inner-cell shape (a). A zoomed view of the trajectories at the equator is shown in (b). The width of the resonance loop is ~0.5 mm.

CONCLUSION

A MP phenomenon is presently limiting C75 cavities from reliably achieving the target E_{acc}-value during RF test qualification in a vertical cryostat. The shift of the MP barrier from ~21 MV/m to ~17 MV/m during testing is an unexpected feature of this phenomenon. The barrier at ~21 MV/m was found to be at the equator of the center cell, the one at ~17 MV/m was found to be ~2 cm away from the equator. The fact that the shifting of the MP barrier could be reproduced after a thermal cycle to 20 K may suggest that magnetic flux, locally trapped at the location of the MP-induced quenches, may be involved. No strong correlation was found so far between the occurrence of this phenomenon and either the bulk surface treatment method, the geometry of the equator weld-prep or the partial pressure of residual gases in the cavities. Altering the cell shape by mechanical tuning did not have a significant impact on the MP barrier.

MP simulations show the possibility of MP at the equator above ~19 MV/m if the initial energy of the secondary electron was to be 4 eV or higher. The detailed geometry of the equatorial weld might impact this prediction, even though the inner surface, including the equator area, is smoothened by CBP.

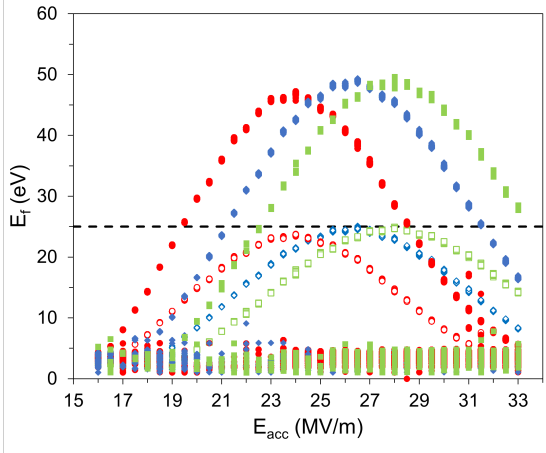

Figure 10: Final impact energy of electrons making 20 impacts to the surface as a function of E_{acc} calculated with ACE3P for the end-cell on the fundamental power coupler side (blue symbols), center cell (red symbols) and for the end-cell on the higher order mode side (green symbols). Solid and empty symbols are for an initial energy of the secondary electron of 4 eV and 2 eV, respectively. The dashed line represents the threshold for SEY > 1 for unbaked Nb.

An R&D effort is currently underway to apply the plasma processing technique [16] to reduce the SEY of the Nb surface in-situ as a possible method to reduce the occurrence of the MP in C75 cavities installed in CEBAF.

ACKNOWLEDGMENTS

We would like to thank the SRF Cavity Production and Test and Measurement Groups at Jefferson Lab for the cavity preparation and cryogenic RF testing. We would also like to thank J. Guo and G.-T. Park for useful discussion on MP simulations.

REFERENCES

[1] R. A. Rimmer *et al.*, "Upgraded Cavities for the CEBAF Cryomodule Rework Program", in *Proc. SRF'17*, Lanzhou, China, Jul. 2017, pp. 168–172. doi:10.18429/JACoW-SRF2017-MOPB049

[2] M. McCaughan, K. Davis, M. Drury, G. Ciovati, and A. Reilly, "Commissioning of the Second JLAB C75 Cryomodule & Performance Evaluation of Installed C-75 Cavities", presented at SRF'23, Grand Rapids, MI, USA, Jun. 2023, paper MOIAA05, this conference.

[3] R. A. Rimmer *et al.*, "The JLAB Ampere-class Cryomodule Conceptual Design", in *Proc. EPAC'06*, Edinburgh, UK, Jun. 2006, paper MOPCH182, pp. 490–492.

[4] H. Wang, R. A. Rimmer, and G. Wu, "Elliptical Cavity Shape Optimization for Acceleration and HOM Damping", in *Proc.*

ISBN: 978-3-95450-234-9 ISSN: 2673-5504 doi:10.18429/JACoW-SRF2023-WEPWB049

PAC'05, Knoxville, TN, USA, May 2005, paper TPPT086, pp. 4191–4193.

[5] G. Wu, M. Stirbet, H. Wang, R. Rimmer, and E. Donoghue, "Multipacting Analysis for JLAB Ampere Class Cavities", in *Proc. SRF'05*, Ithaca, NY, USA, Jul. 2005, pp. 300–302.

[6] P. Kneisel *et al.*, "Preliminary Results from Prototype Niobium Cavities for the JLab Ampere-Class FEL", in *Proc. PAC'07*, Albuquerque, NM, USA, Jun. 2007, pp. 2487–2489.

[7] F. Marhauser *et al.*, "Status and Test Results of High Current 5-cell SRF Cavities Developed at JLAB", in *Proc. EPAC'08*, Genoa, Italy, Jun. 2008, paper MOPP140, pp. 886–888.

[8] R. A. Rimmer *et al.*, "Recent Progress on High-Current SRF Cavities at JLab", in *Proc. IPAC'10*, Kyoto, Japan, May 2010, paper WEPEC076, pp. 3052–3054.

[9] G. Ciovati *et al.*, "Cavity Production and Testing of the First C75 Cryomodule for CEBAF",, in *Proc. SRF'21*, East Lansing, MI, USA, Jun.-Jul. 2021, pp. 250–254. doi:10.18429/JACoW-SRF2021-MOPCAV001

[10] U. Pudasaini, G.V. Eremeev, M.J. Kelley, and C.E. Reece, "Recent Developments of Nb_3Sn at Jefferson Lab for SRF Accelerator Application", in *Proc. NAPAC'19*, Lansing, MI, USA, Sep. 2019, pp. 713–716. doi:10.18429/JACoW-NAPAC2019-WEPLM52

[11] S. Berry *et al.*, "Cleanliness and Vacuum Acceptance Tests for the UHV Cavity String of the XFEL Linac", in *Proc. SRF'15*, Whistler, Canada, Sep. 2015, paper MOPB118, pp. 452–456.

[12] G. Myneni *et al.*, "Medium grain niobium SRF cavity production technology for science frontiers and accelerator applications", *J. Instrum.*, vol. 18, p. T04005, Apr. 2023. doi:10.1088/1748-0221/18/04/T04005

[13] FishPact, https://code.google.com/archive/p/fishpact/downloads

[14] R. Calder, G. Dominichini, and N. Hilleret, "Influence of various vacuum surface treatments on the secondary electron yield of niobium", *Nucl. Instrum. Methods Phys. Res., Sect. B*, vol. 13, pp. 631–636, Mar. 1986. doi:10.1016/0168-583X(86)90581-1

[15] L. Xiao, L. Ge, Z. Li, and C.-K. Ng, "Advances in multiphysics modeling for parallel finite element code suite ACE3P", *IEEE J. Multiscale Multiphys. Comput. Tech*, vol. 4, pp. 298–306, Nov. 2019. doi:10.1109/JMMCT.2019.2954946

[16] T. Powers, N. C. Brock, and T. D. Ganey, "In Situ Plasma Processing of Superconducting Cavities at JLab", in *Proc. NAPAC'22*, Albuquerque, NM, USA, Aug. 2022, pp. 22–25. doi:10.18429/JACoW-NAPAC2022-MOYE5